Sensors and Materials, Vol. 37, No. 5 (2025) 1949–1957
MYU Tokyo

S & M 4032

Alpha Particle Measurement of Radioactive Substances in Nitric Acid Using a Single-crystal CVD Diamond Radiation Detector

Kengo Oda,[1*] Junichi H. Kaneko,[1] Akiyoshi Chayahara,[2] Takehiro Shimaoka,[2]
Hideaki Yamada,[2] Hitoshi Umezawa,[3] and Naohisa Hoshikawa[1,4]

[1]Graduate School of Engineering, Hokkaido University,
Kita 13 Nishi 8, Kita-ku, Sapporo, Hokkaido 060-8628, Japan
[2]National Institute of Advanced Industrial Science and Technology (AIST),
1-8-31 Midorigaoka, Ikeda, Osaka 563-8577, Japan
[3]National Institute of Advanced Industrial Science and Technology (AIST),
1-1-1 Umezono, Tsukuba, Ibaraki 305-8568, Japan
[4]Ookuma Diamond Device Co., Ltd.,
Hokudai Business Spring, Nishi 12-2, Kita 21, Kita-ku, Sapporo, Hokkaido, Japan

(Received January 6, 2025; accepted April 23, 2025)

Keywords: single-crystal CVD diamond, radiation detector, alpha particle, nitric acid, nuclear fuel reprocessing

We attempted to measure α-particles emitted by radioactive substances present in nitric acid using a single-crystal CVD diamond radiation detector, which allows for the acquisition of detailed energy information, in place of conventionally used polycrystalline diamonds and other materials, primarily designed for use in nuclear fuel reprocessing facilities. Using a 10-mm-square single-crystal CVD diamond substrate, we grew a single-crystal CVD diamond as the detector by the direct wafer method. A Ti/Au ohmic-contact anode electrode and a Pt ohmic-contact cathode electrode were formed on opposite sides of a 66-μm-thick freestanding single-crystal CVD diamond membrane by evaporation. The charge collection efficiency of the fabricated detector for 5.486 MeV α-particles was 99.1% for both holes and electrons, with energy resolutions of 0.55% and 0.54%, respectively. Instead of using the Pt cathode electrode, 5 mol/L nitric acid was used, and the α-particle spectrum from thorium oxide diffused in nitric acid was measured. The rise time of the preamplifier output signal was approximately 30 ns, and the high energy resolution enabled us to obtain a spectrum that reflected more detailed energy structures than when using conventional polycrystalline diamond detectors. Continuous measurements over 72 h confirmed the minimal influence from γ-rays.

1. Introduction

Diamond is a semiconductor with a wide bandgap of 5.5 eV, possessing excellent characteristics such as radiation resistance,(1,2) high-temperature operation,(3,4) near-biological

---

[*] Corresponding author: e-mail: odahokudaikengo64@eis.hokudai.ac.jp

https://doi.org/10.18494/SAM5526

ISSN 0914-4935 © MYU K.K.
https://myukk.org/

equivalence,(5,6) solar-blind properties,(7,8) high saturation drift velocity,(9,10) and high breakdown strength.(11) The potential application of diamond to radiation measurements was demonstrated in pioneering research by Kozlov *et al.* in the 1970s using natural single-crystal diamonds.(12–15) Particularly with the advancement of microwave plasma CVD,(16) polycrystalline diamonds(17–19) with excellent charge carrier transport properties and single-crystal CVD diamonds for energy spectrometer-grade applications have emerged.(20,21) Furthermore, with the commercialization of detector-grade single-crystal CVD diamonds, their use has expanded across various fields.

One of the applications of diamond radiation detectors is nuclear fuel reprocessing.(22) In this application, α-particles from dissolved nuclear fuel in nitric acid are measured, which is used for determining the ratio of ^{240}Pu to ^{239}Pu, monitoring the concentration of actinides in the solution, and tracking the material composition. The application of diamonds in this field was reported by Kozlov *et al.*,(23) using natural single-crystal diamonds. Bergonzo *et al.* used polycrystalline diamond synthesized on a silicon substrate as a detector, which is employed in actual nuclear fuel reprocessing facilities.(24) Similarly, the application of 4H-SiC semiconductor detectors, which also exhibit excellent radiation resistance, has also been reported.(25,26)

The recent expansion of the synthetic gemstone market and the increasing demand for semiconductor device substrates have driven the scaling up of single-crystal diamond substrates, as well as the growth of energy spectrometers.(27) In this study, we measured α-particles from radioactive materials in nitric acid using a single-crystal CVD diamond as a radiation detector, with its future use in nuclear fuel reprocessing facilities in mind.

2. Materials and Methods

2.1 Crystal growth of single-crystal CVD diamond and detector fabrication

Since the sensitive area of detectors actually used in nuclear fuel reprocessing facilities is approximately 7 mm Φ, a 10-mm-square single-crystal CVD diamond substrate manufactured by EDP Corporation was used as the base substrate, as shown in Fig. 1(a). Figure 1(b) shows numerous structural defects in the crystal under a polarized light microscope. To reduce the occurrence of residual stress caused by structural defects and impurities, an epitaxial growth layer approximately 50 μm thick was stacked on the base substrate. This crystal has a tilt of about 3° with respect to the [110] direction of the (001) plane.

The diamond as the detector was obtained from a synthetic diamond grown by the direct wafer method(28) to form a freestanding membrane. Carbon ions were implanted into the substrate in advance, and an ion implantation layer was formed at a depth of 1.6 μm from the surface. Using this ion-implanted substrate, we epitaxially grew the diamond as the detector using a microwave plasma CVD system (Cornes Technology AX5250). The synthesis conditions were as follows: substrate temperature, 870°C; gas pressure, 110 Torr; CH_4 concentration, 1.0%; and O_2 concentration, 0.5%.(29) Figure 1(c) shows a laser microscopy image of the synthesized diamond as the detector. Owing to plasma asymmetry during synthesis, etching on the right side of the substrate was stronger, resulting in increased surface roughness. After synthesis, the ion implantation layer was removed by electrochemical etching, and a freestanding single-crystal

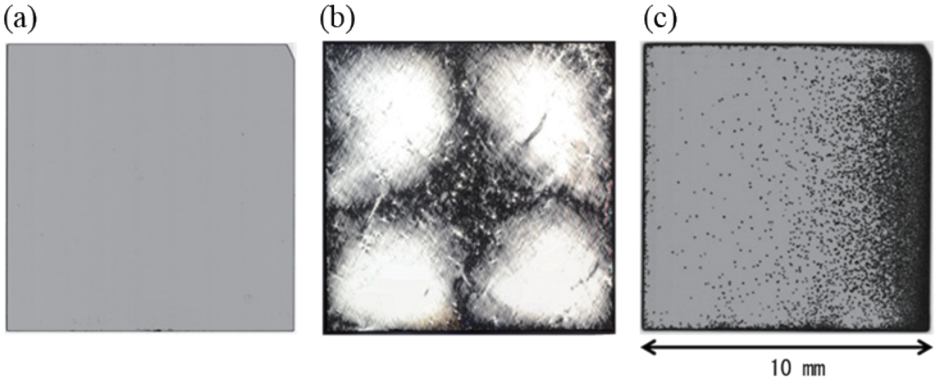

Fig. 1. (a) Laser microscopy image of the single-crystal CVD substrate manufactured by EDP Corporation, (b) polarized light microscopy image of the diamond substrate used, and (c) laser microscopy image of the synthesized diamond as the detector.

CVD diamond membrane was obtained. The damage layer on the substrate separation surface was removed by ion-beam irradiation. The thickness of the freestanding single-crystal CVD diamond membrane was 66 µm. A Ti/Au ohmic-contact anode electrode and a Pt ohmic-contact cathode electrode were formed on opposite sides of a 66-µm-thick freestanding single-crystal CVD diamond membrane by evaporation. The thickness of each electrode was approximately 100 nm.

2.2 Experimental setup

To evaluate the basic performance of the detector, the freestanding single-crystal CVD diamond membrane with Ti/Au–Pt electrodes formed on both sides was mounted in the detector housing. The Ti/Au ohmic-contact anode electrode was connected to the SMA receptacle, while the Pt ohmic-contact cathode electrode was connected to ground. *I–V* characteristic and α-particle energy spectrum measurements were performed in a vacuum at room temperature. The *I–V* measurements were conducted using a Keithley 237 source measurement unit. For α-particle measurements, 5.486 MeV α-particles from a ^{241}Am source were used. For spectrum measurements, the following equipment was used: preamplifier (ORTEC 142A), main amplifier (ORTEC 672), high-voltage power supply (ORTEC 428), pulser (ORTEC 419), and MCA (YOKOGAWA WE7562). Signals were observed using a TELEDYNE LECROY Waverunner LT-584.

A device with the cross-sectional structure shown in Fig. 2 was fabricated and evaluated for measuring α-particles from radioactive substances in a solution. The device, constructed from acrylic to allow the observation of its interior, housed a diamond with electrodes. A 5 mol/L nitric acid solution was prepared by diluting 13 mol/L nitric acid with deionized water at a ratio of 1:1.6 in a 10 mL glass beaker. The solution chamber on the cathode electrode side, with a volume of 0.42 cm^3, was filled with 5 mol/L nitric acid, which functioned as a substitute for the Pt cathode electrode, and thorium oxide was dispersed into the solution. For structural rigidity,

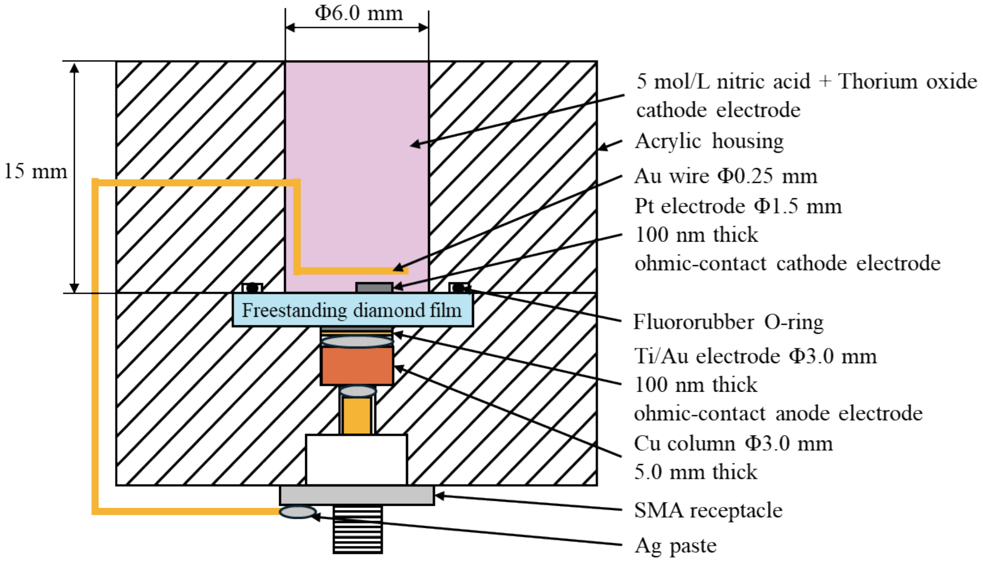

Fig. 2. (Color online) Overview diagram of the evaluation device.

the diamond was attached to the acrylic container using epoxy resin, and a fluororubber O-ring, known for its excellent acid resistance, was used to seal the solution. Thorium oxide was employed as the α-particle source. Although actual nuclear fuel reprocessing is conducted at approximately 60 °C, measurements in this study were performed at room temperature owing to the limitations of the experimental setup. Prior to the nitric acid experiments, the system's integrity was verified using a saturated saline solution. The measurement setup used the same equipment described earlier for *I*–*V* measurements and α-particle detection.

3. Experimental Results and Discussion

3.1 Basic performance of diamond detector

Figure 3 shows an example of the *I*–*V* characteristic measurement of the single-crystal CVD diamond detector with Ti/Au–Pt electrodes. The applied voltage during the *I*–*V* characteristic measurement ranged from −300 to +300 V. The leakage currents were approximately 7 pA at both −264 and +264 V, confirming that the necessary voltage for measurements can be applied.

Figure 4 shows an example of the α-particle energy spectrum measured in a vacuum. The notation of holes and electrons in the figure indicates that the measurements were conducted under conditions where the drift of either holes or electrons became the dominant signal formation mechanism by changing the polarity of the bias voltage applied to the detector. The range of 5.486 MeV α-particles in the diamond was 13–14 μm, and since the crystal thickness was 66 μm, complete separation was not achieved. The bias voltages applied to the detector were −264 and +264 V for holes and electrons, respectively. The energy resolutions ($\Delta E/E$) were 0.55% for holes and 0.54% for electrons. The charge collection efficiency of the diamond

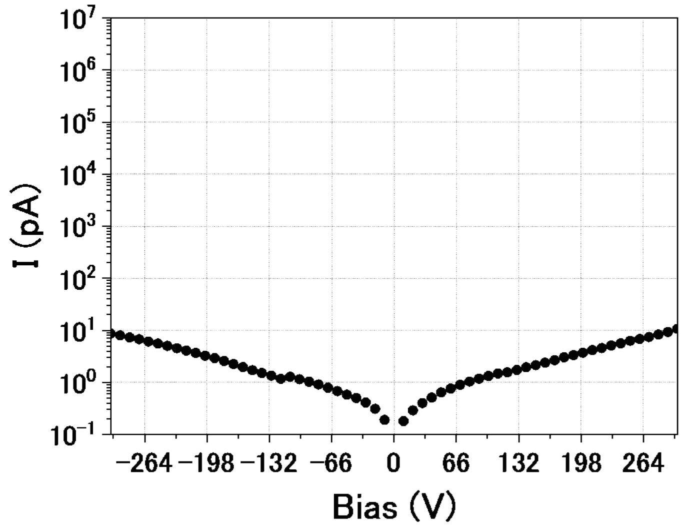

Fig. 3. *I–V* characteristics of the fabricated detector with the Ti/Au-Pt electrodes.

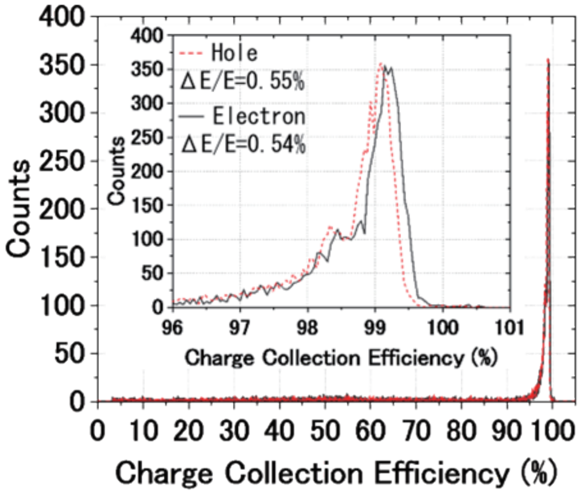

Fig. 4. (Color online) Measurement of the 5.486 MeV α-particle energy spectrum using the fabricated detector with the Ti/Au-Pt electrodes.

detector shown on the horizontal axis in Fig. 4 was determined by comparing the results of a similar measurement performed using a silicon semiconductor detector with a charge collection efficiency of nearly 100%. This comparison was made using the average electron–hole pair creation energies for the silicon and diamond detectors, which are 3.62 eV for silicon and 13.1 eV for diamond. Depending on the value of the electron–hole pair average generation energy of the diamond used here, the charge collection efficiency may exceed 100%. The shaping time of the main amplifier was 1.0 μs. The charge collection efficiency was 99.1% for both holes and electrons. When using high-pressure, high-temperature synthesized IIa-type single-crystal diamonds with excellent crystallinity as the base substrate, the charge collection efficiency often slightly exceeds 100%,(30) suggesting that the crystallinity of the base substrate used may have influenced the results.

3.2 Results of α-particle measurement in solution

Figure 5 shows an example of the *I–V* characteristic measurement of the single-crystal CVD diamond detector, measured using 5 mol/L nitric acid and a saturated saline solution as the cathode electrodes. The applied voltage during the *I–V* characteristic measurement ranged from −300 to +300 V. In both cases of 5 mol/L nitric acid and saturated saline, a large leakage current flows on the positive side, and the limiter is applied. On the negative side, the leakage current was 4 pA for 5 mol/L nitric acid and 1 pA for the saturated saline solution at −33 V, confirming that the measurement is sufficiently feasible.

Figure 6 shows a comparison of the preamplifier output signals when using 5 mol/L nitric acid and a saturated saline solution. In both cases, signals with a rise time of approximately 30 ns were observed. The resistance of the 5 mol/L nitric acid was between 3 and 8 MΩ, whereas the resistance of the saturated saline solution ranged from 30 to 168 kΩ. The resistance of the solution, prepared in a beaker, was measured using a digital multimeter, with probe separation ranging from 1 to 22 mm.

Figure 7 shows an example of the α-particle energy spectrum measurement from thorium oxide in 5 mol/L nitric acid and a saturated saline solution. The applied voltage was −33 V. Owing to the low α-particle emission rate from thorium oxide, the counting rate was about 0.02 cps, and the measurement took 72 h. It was confirmed that stable α-particle measurements can be performed with the single-crystal diamond detector. The horizontal axis in Fig. 7 is calibrated

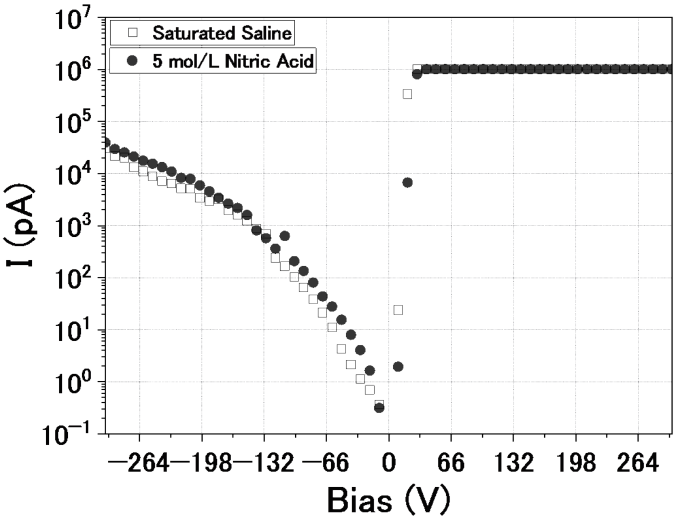

Fig. 5. *I–V* characteristic when 5 mol/L nitric acid and saturated saline solution are injected into the solution chamber.

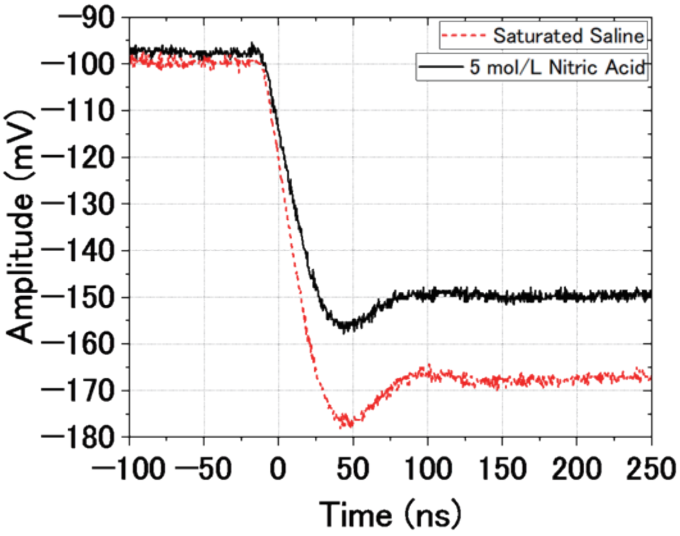

Fig. 6. (Color online) Preamplifier output signals when using 5 mol/L nitric acid and a saturated saline solution.

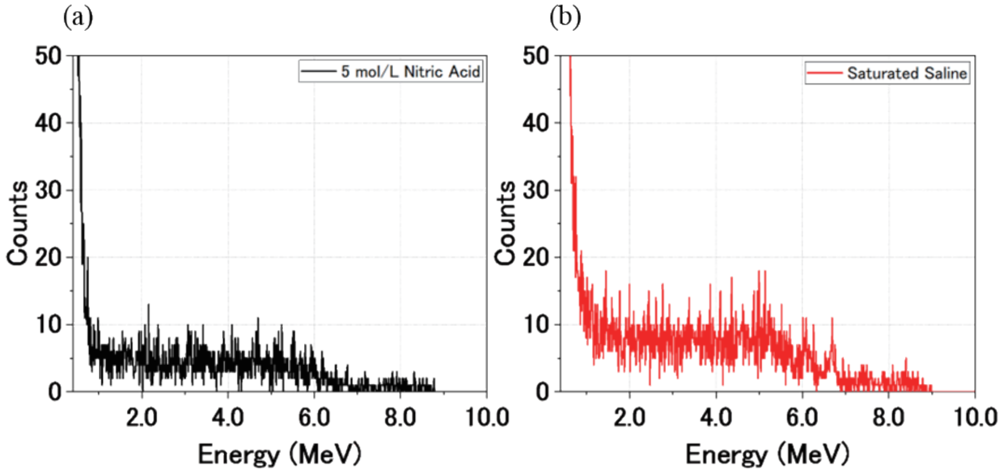

Fig. 7. (Color online) Alpha-particle spectrum measurement from thorium oxide in (a) 5 mol/L nitric acid and (b) saturated saline solution (measurement time, 72 h; 0.02 cps).

using the 5.486 MeV α-particle in a vacuum. The α-particles from the thorium oxide primarily originate from the 6.228 MeV α-particles of ^{220}Rn and the 6.779 MeV α-particles of the accompanying ^{216}Po. In the α-particle spectrum of the saturated saline solution, peaks at around 6.1 and 6.7 MeV were observed, and since the energies generally matched, it is considered that the peaks originated from the α-particles of ^{220}Rn and ^{216}Po.

Compared with the spectra obtained using polycrystalline diamond, the influence of the energy distribution of the emitted α-particles is evident. The counting rate in the 7.0 to 9.0 MeV range, which is considered to originate from the 8.785 MeV α-particles of ^{212}Po, is lower than that for lower-energy α-particles. Thorium oxide emits a significant quantity of γ-rays, but it was also confirmed that the thin detector has no significant effect.

Since the evaluation device is made of acrylic, measurements at 60 °C, as required for actual nuclear fuel reprocessing applications, were not conducted. However, considering that α-particle energy measurements have been successfully performed at 500 °C using a high-pressure, high-temperature IIa-type diamond single-crystal substrate with excellent crystallinity,(31) it is believed that the diamond detector will have no issues operating at 60 °C.

4. Conclusion

The 10-mm-square single-crystal CVD diamond substrate was used, and a single-crystal CVD diamond as the detector was synthesized by the direct wafer method. Ti/Au–Pt electrodes were formed on the 66-μm-thick freestanding single-crystal CVD diamond membrane. The charge collection efficiency of the fabricated detector for 5.486 MeV α-particles was approximately 99.1%, and the energy resolution was around 0.54%. Subsequently, the α-particle spectrum was measured using a solution containing thorium oxide in 5 mol/L nitric acid as the cathode electrode. The rise time of the preamplifier output signal was approximately 30 ns, and as expected from the high energy resolution when the cathode electrode was Pt, even when the cathode electrode was 5 mol/L nitric acid, the spectrum reflected more detailed energy structures than in the case of using conventional polycrystalline diamond detectors. Continuous measurements were conducted for 72 h, and the influence of γ-rays was found to be minimal. Owing to the limitations of the evaluation equipment, the measurements were confined to room temperature. However, since diamonds can be used to fabricate detectors capable of measuring energy spectra up to around 500 °C, there should be no significant issues for practical use.

In this case, the single-crystal CVD diamond substrate with inferior crystallinity was used. However, when applying it to practical devices, 12-mm-square substrates of high-pressure, high-temperature-synthesized IIa type with excellent crystallinity can also be used. Considering factors such as long-term stability, it is desirable to use substrates with superior crystallinity.

Acknowledgments

A part of this research includes content supported by the Fukushima Prefecture Regional Revitalization Practical Development Promotion Project Grant.

References

1 C. Bauer, I. Baumann, C. Colledani, J. Conway, P. Delpierre, F. Djama, W. Dulinski, A. Fallou, K. K. Gan, R. S. Gilmore, E. Grigoriev, G. Hallewell, S. Han, T. Hessing, K. Honschied, J. Hrubec, D. Husson, H. Kagan, D. Kania, R. Kass, W. Kinnison, K. T. Knopfle, M. Krammer, T. J. Llewellyn, P. F. Manfredi, L. S. Pan, H. Pernegger, M. Pernicka, R. Plano, V. Re, S. Roe, A. Rudge, M. Schaeffer, S. Schnetzer, S. Somalwar, V. Speziali, R. Stone, R. J. Tapper, R. Tesarek, W. Trischuk, R. Turchetta, G. B. Thomson, R. Wagner, P. Weilhammer, C. White, H. Ziock, and M. Zoeller: Nucl. Instrum. Methods Phys. Res., Sect. A **367** (1995) 207. https://doi.org/10.1016/0168-9002(95)00545-5

2 W. D. Boer, J. Bol, A. Furgeri, S. Muller, C. Sander, E. Berdermann, M. Pomorski, and M. Huhtinen: Phys. Status Solidi A **204** (2007) 3004. https://doi.org/10.1002/pssa.200776327

3 M. Tsubota, J. H. Kaneko, D. Miyazaki, T. Shimaoka, K. Ueno, T. Tadokoro, A. Chayahara, H. Watanabe, Y. Kato, S. Shikata, and H. Kuwabara: Nucl. Instrum. Methods Phys. Res., Sect. A **789** (2015) 50. http://doi.org/10.1016/j.nima.2015.04.002

4 A. Kumar, A. Kumar, A. Topkar, and D. Das: Nucl. Instrum. Methods Phys. Res., Sect. A **858** (2017) 12. https://doi.org/10.1016/j.nima.2017.03.033

5 B. Planskoy: Phys. Med. Biol. **25** (1980) 519. https://doi.org/10.1088/0031-9155/25/3/011

6 A. J. Whitehead, R. Airey, C.M. Buttar, J. Conway, G. Hill, S. Ramkumar, G. A. Scarsbrook, R. S. Sussmann, and S. Walker: Nucl. Instrum. Methods Phys. Res., Sect. A **460** (2001) 20. https://doi.org/10.1016/S0168-9002(00)01090-1

7 F. Foulon, P. Bergonzo, C. Borel, R. D. Marshall, C. Jany, L. Besombes, A. Brambilla, D. Riedel, L. Museur, and M. C. Castex: J. Appl. Phys. **84** (1998) 5331. https://doi.org/10.1063/1.368782

8 Y. Koide, M. Y. Liao, and J. Alvarez: Diamond Relat. Mater. **15** (2006) 1962. https://doi.org/10.1016/j.diamond.2006.08.009

9 M. Pomorski, E. Berdermann, M. Ciobanu, A. Martemyianov, P. Moritz, M. Rebisz, and B. Marczewska: Phys. Status Solidi A **202** (2005) 2199. https://doi.org/10.1002/pssa.200561929

10 M. Pomorski, E. Berdermann, A. Caragheorgheopol, M. Ciobanu, M. Kis, A. Martemiyanov, C. Nebel, and P. Moritz: Phys. Status Solidi A **203** (2006) 3152. https://doi.org/10.1002/pssa.200671127

11 C. J. H Wort and R. S. Balmer: Mater. Today **11** (2008) 22. https://doi.org/10.1016/S1369-7021(07)70349-8

12 E. A. Korova and S. F. Kozlov: Sov. Phys. Semiconductors-Ussr **4** (1971) 1600.

13 S. F. Kozlov, E. Belcarz, M. Hageali, R. Stuck, and P. Siffert: Nucl. Instrum. Methods **117** (1974) 277. https://doi.org/10.1016/0029-554X(74)90410-8

14 S. F. Kozlov, R. Stuck, M. Hageali, and P. Siffert: IEEE Trans. Nucl. Sci. **NS22** (1975) 160. https://doi.org/10.1109/TNS.1975.4327634

15 C. Canali, E. Gatti, S. F. Kozliv, P. F. Manfredi, C. Manfredotti, F. Nava, and A. Quirini: Nucl. Instrum. Methods **160** (1979) 73. https://doi.org/10.1016/0029-554X(79)90167-8

16 M. Kamo, Y. Sato, S. Matsumoto, and N. Setaka: J. Cryst. Growth **62** (1983) 642. https://doi.org/10.1016/0022-0248(83)90411-6

17 M. Franklin, A. Fry, K. K. Gan, S. Han, H. Kagan, S. Kanda, D. Kania, R. Kass, S. K. Kim, R. Malchow, F. Morrow, S. Olsen, W. F. Palmer, L. S. Pan, F. Sannes, S. Schnetzer, R. Stone, Y. Sugimoto, G. B. Thomson, C. White, and S. Zhao: Nucl. Instrum. Methods Phys. Res., Sect. A **315** (1992) 39. https://doi.org/10.1016/0168-9002(92)90677-V

18 F. Foulon, T. Pochet, E. Gheeraert, and A. Deneuville: IEEE Trans. Nucl. Sci. **41** (1994) 927. https://doi.org/10.1109/23.322833

19 E. K. Souw and R. J. Meilunas: Nucl. Instrum. Methods Phys. Res., Sect. A **400** (1997) 69. https://doi.org/10.1016/S0168-9002(97)00963-7

20 J. H. Kaneko, T. Tanaka, T. Imai, Y. Tanimura, M. Katagiri, T. Nishitani, H. Takeuchi, T. Sawamura, and T. Iida: Nucl. Instrum. Methods Phys. Res., Sect. A **505** (2003) 187. https://doi.org/10.1016/S0168-9002(03)01048-9

21 G. J. Schmid, J. A Koch, R. A. Lerche, and M. J. Moran: Nucl. Instrum. Methods Phys. Res., Sect. A **527** (2004) 554. https://doi.org/10.1016/j.nima.2004.03.199

22 J. B. Coble, S. E. Skutnik, S. N. Gillam, and M. P. Cooper: Nucl. Technol. **206** (2020) 1803. https://doi.org/10.1080/00295450.2020.1724728

23 S. F. Kozlov, E. A. Konorova, M. I. Krapivin, V. A. Nadein, and V. G. Yudina: IEEE Trans. Nucl. Sci. **24** (1977) 242. https://ieeexplore.ieee.org/stamp/stamp.jsp?arnumber=4328681

24 P. Bergonzo, F. Foulon, A. Brambilla, D. Tromson, C. Jany, and S. Haan: Diamond Relat. Mater. **9** (2000) 1003. https://doi.org/10.1016/S0925-9635(99)00257-5

25 A. R. Zelaski: "Development of a Silicon Carbide Schottky Diode Detector for Use in Determining Actinide Inventories Based on Alpha Particle Spectroscopy", Master's Thesis, The Ohio State University (2011). http://rave.ohiolink.edu/etdc/view?acc_num=osu1316486528

26 T. Garcia: "Fabrication, Characterization and Simulation of 4H-SiC Schottky Diode Alpha Particle Detectors for Pyroprocessing Actinide Monitoring", Ph.D. Thesis, The Ohio State University (2014). https://ui.adsabs.harvard.edu/abs/2014PhDT.......282G/abstract

27 S. Hirano, J. H. Kaneko, T. Hanada, S. Ito, T. Shimaoka, H. Shimmyo, M. Tsubota, A. Chayahara, Y. Mokuno, and H. Umezawa: Phys. Status Solidi A **215** (2018) 1800333. https://doi.org/10.1002/pssa.201800333

28 Y. Mokuno, A. Chayahara, and H. Yamada: Diamond Relat. Mater. **17** (2008) 415. https://doi.org/10.1016/j.diamond.2007.12.058

29 K. Oda, J. H. Kaneko, A. Chayahara, H. Watanabe, H. Umezawa, and Y. Kobayakawa: Diamond Relat. Mater. **148** (2024) 111441. https://doi.org/10.1016/j.diamond.2024.111441

30 T. Shimaoka, J. H. Kankeko, M. Tsubota, H. Shimmyo, H. Watanabe, A. Chayahara, H. Umezawa, and S. Shikata: Europhys. Lett. **113** (2016) 62001. https://doi.org/10.1002/pssa.201600195

31 T. Hanada, J. H. Kaneko, T. Shimaoka, A. Chayahara, H. Watanabe, K. Yukako, H. Umezawa, and Y. Mokuno: New Diamond **34** (2018) 36 (in Japanese). https://jndf.org/katsudo/kaishi/backnumber/kaishi-130.html